BIOCHEMISTRY
including biophysical chemistry & molecular biology

Article

pubs.acs.org/biochemistry

Mechanism of the Chaperone-like and Antichaperone Activities of Amyloid Fibrils of Peptides from αA-Crystallin

Sayuri Fukuhara, Tatsutoshi Nishigaki, Keisuke Miyata, Nobuhiko Tsuchiya, Tomonori Waku, and Naoki Tanaka*

Department of Biomolecular Engineering, Kyoto Institute of Technology, Matsugasaki, Sakyo, Kyoto 606-8585, Japan

Supporting Information

ABSTRACT: The amyloid fibril of a fragment of the substrate binding site of αA-crystallin (αAC(71−88)) exhibited chaperone-like activity by suppressing the aggregation of alcohol dehydrogenase (ADH) and luciferase. By contrast, the amyloid fibril of the cytotoxic fragment of amyloid β protein (Aβ(25−35)) facilitated the aggregation of the same proteins. We have determined the zeta potential of the amyloid fibril by measuring their electrophoretic mobility to study the effects of the surface charge on the modulation of protein aggregation. The αAC(71−88) amyloid possesses a large negative zeta potential value which is unaffected by the binding of the negatively charged ADH, indicating that the αAC(71−88) amyloid is stable as a colloidal dispersion. By contrast, the Aβ(25−35) amyloid possesses a low zeta potential value, which was significantly reduced with the binding of the negatively charged ADH. The canceling of the surface charge of the amyloid fibril upon substrate binding reduces colloidal stability and thereby facilitates protein aggregation. These results indicate that one of the key factors determining whether amyloid fibrils display chaperone-like or antichaperone activity is their electrostatic interaction with the substrate. The surface of the αAC(71−88) amyloid comprises a hydrophobic environment, and the chaperone-like activity of the αAC(71−88) amyloid is best explained by the reversible substrate binding driven by hydrophobic interactions. On the basis of these findings, we designed variants of amyloid fibrils of αAC(71−88) that prevent protein aggregation associated with neurodegenerative disorders.

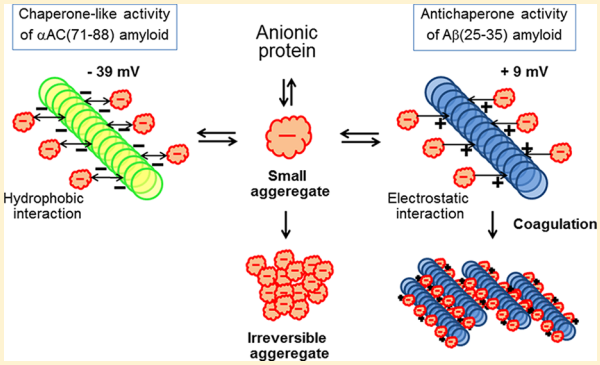

Amyloid fibrils are self-assembled, highly ordered linear aggregates of a soluble protein or peptide. The formation of amyloid fibrils is associated with protein misfolding diseases, including neurodegenerative disorders such as Alzheimer's disease and Parkinson's disease.[1] The presence of amyloid fibrils is one of the characteristic features of these diseases, although soluble oligomers are regarded as more cytotoxic than fibrillar aggregate.[2] The use of α-crystallin, a member of the small heat shock superfamily of proteins, to prevent protein aggregation and toxicity has been explored.[3] The chaperone-like function of α-crystallin was first recognized when it was found to prevent protein aggregation in the eye lens and thereby maintain transparency.[4] α-Crystallin consists of two closely related subunits A and B (20 kDa each), which form highly heterogeneous multimers with a molecular mass of ca. 800 kDa. Approximately 60−70% of the α-crystallin polypeptide is arranged in β-strands with very little or no α-helix. The crystal structures of the N- and C-terminal truncated αA-crystallin and αB-crystallin show that they adopt an immunoglobulin-like β-sandwich fold formed from seven β-strands.[5]

Hydrophobic interaction has been proposed to be involved in substrate binding of α-crystallin because the chaperone-like activity of α-crystallin correlates with the extent of hydrophobicity at its molecular surface.[6] Interestingly, synthetic peptides that correspond to the hydrophobic substrate binding site of α-crystallin[7,8] prevent the aggregation of various proteins.[9−11] The chaperone-like activity was first observed in a peptide comprising amino acid residues 70−88 of αA-crystallin (αAC(70−88), KFVIFLDVKHFSPEDLTVK).[9] The chaperone-like activity was also displayed by the slightly shorter peptide αAC(71−88). However, removal of one further amino acid from the N-terminal end of the peptide (i.e., to give αAC(72−88)) significantly reduced chaperone-like activity, suggesting F71 plays a vital role in the interaction.

In a previous study, we investigated the effects of αAC(71−88) on the kinetics and morphology of protein aggregation to reveal the mechanism of its chaperone-like activity.[12] At elevated temperature, the conformation of αAC(71−88) changed from a random coil to one rich in the β-sheet followed by the formation of amyloid fibrils (Figure 1a). The FVIFLD sequence is commonly found in the short variants of αAC(71−88) with the ability to form amyloid fibrils, indicating that this sequence is important for the amyloid fibril formation.

Received: April 2, 2012
Revised: June 12, 2012
Published: June 14, 2012

dx.doi.org/10.1021/bi3004236 | *Biochemistry* 2012, 51, 5394−5401

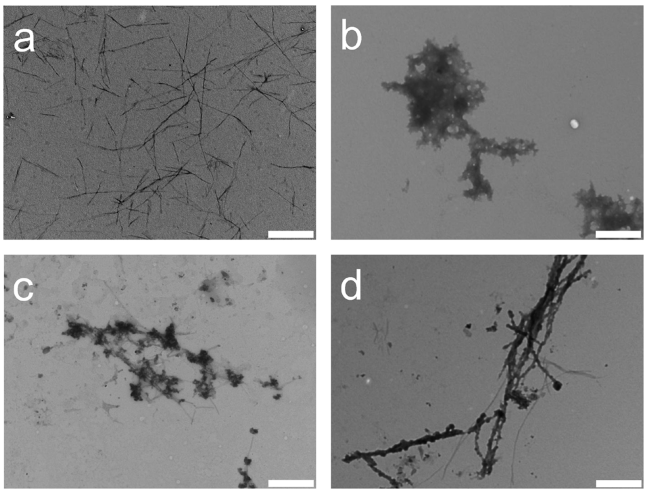

Figure 1. TEM images of the aggregates. (a) Amyloid fibrils obtained by incubation of αAC(71−88) (10 μg/mL) at 60 °C for 1 h. (b) Aggregate obtained after incubation of ADH (150 μg/mL) at 44 °C for 1 h. (c) Aggregate obtained after incubation of a mixture of ADH (150 μg/mL) and αAC(71−88) amyloid (10 μg/mL) at 44 °C for 1 h. (d) Aggregate obtained after the incubation of a mixture of luciferase (50 μg/mL) and the αAC(70−88) amyloid (6 μg/mL) at 37 °C for 15 min. The scale bars are 1 μm.

Removal of F71 from αAC(71−88) not only reduced the chaperone-like activity of the peptide but also decreased its propensity to form amyloid fibrils, suggesting that the fibril formation of αAC(71−88) is related to its chaperone-like activity. By contrast, the amyloid fibrils of other peptides have been reported to facilitate protein aggregation.[13−15] Indeed, a detailed mechanism has been proposed for the cytotoxic fragment of amyloid β protein Aβ(25−35).[13] The Aβ(25−35) amyloid has a net positive charge at neutral pH and thus interacts preferably with acidic proteins by electrostatic interactions to facilitate aggregation. These functions of the amyloid fibril are referred to as antichaperone because they are opposite in direction to those of the molecular chaperone system.

In the present study, we have analyzed the electrophoretic motion of the amyloid fibrils to reveal the mechanism by which they modulate protein aggregation. The zeta potential of the amyloid fibrils was calculated from their electrophoretic mobility. These results indicated that substrate binding through electrostatic attraction reduces the colloidal stability[16,17] of the amyloid fibrils, thereby allowing them to exhibit antichaperone activity. The chaperone-like activity of αAC(71−88) amyloid is similar to the mechanism described for the substrate binding domain of molecular chaperones.[18−23] On the basis of these findings, we have designed amyloid fibrils that have the potential to prevent neurodegenerative disorders.

MATERIALS AND METHODS

Materials. Yeast alcohol dehydrogenase (ADH) and hen egg white lysozyme were purchased from Sigma-Aldrich (St Louis, MO), and luciferase was obtained from Promega (Madison, WI). Aβ(1−40) (TFA type) and Aβ(25−35) were obtained from Peptide Institute (Osaka, Japan). All peptides used in this study were synthesized and purified by Genescript (Piscataway, NJ). The purities of the peptides used in this study were >95% according to HPLC and mass spectroscopic analyses. The expression vector for three-repeat microtubule-binding domain (3RMBD) of human brain tau protein was kindly provided by Prof. T. Ishida (Osaka University of Pharmaceutical Science).[24] Gene expression and purification of His-tagged 3RMBD were performed as described previously,[25] except that 8 M urea was included in the lysis buffer.

Protein Aggregation. The heat-induced aggregations of ADH and luciferase were assayed using turbidity measurements by monitoring the absorbance of the protein solution. These assays were conducted in 50 mM sodium phosphate buffer (pH 7.0) containing 100 mM NaCl. A solution of ADH (150 μg/mL) was incubated at 44 °C, and the absorbance at 360 nm was monitored.[9] A solution of luciferase (50 μg/mL) was incubated at 37 °C, and the absorbance at 320 nm was monitored.[13] Heat-induced aggregates of 230 μg/mL lysozyme in 50 mM sodium-phosphate buffer (pH 6.5) were quantified as described previously.[26]

Enzymatic Assay. The enzyme activity of ADH was determined by the oxidation of ethanol using NAD^+ as the electron acceptor. The solution of ADH was diluted 100-fold into the assay buffer, and the generation of NADH from NAD^+ was monitored by measuring the change in absorbance at 340 nm. The luciferase activity was determined using a commercial kit obtained from Promega (Madison, WI). The solution of luciferase was diluted 100-fold into the assay buffer, and the light reaction was monitored using a Genios plate reader (TECAN).

Electrophoretic Mobility Measurement. The electrophoretic mobility of the amyloid fibril was measured by laser microscopy using a Model 502 microscope (Nihon Rufut Co, Ltd., Tokyo, Japan) at 25 °C. The motion of individual amyloid fibrils was visualized using light scattering images generated from a He−Ne laser (630 nm). Digital images of particles in motion captured with a CCD camera were transferred to a PC in order to calculate the electrophoretic mobility. The zeta potential is calculated from Smoluchowski's equation:

$$\mu_e = \frac{\varepsilon\zeta}{\eta}$$

where μ_e is the electrophoretic mobility, ε is the dielectric constant, ζ is the zeta potential, and η is the viscosity.

Dynamic Light Scattering (DLS). The size of heat-induced aggregates of ADH in solution was measured by dynamic light scattering using a DLS 7000 (Otsuka Electronics, Osaka, Japan) at 25 °C. The light source was from a He−Ne laser (630 nm) set at an angle of 45°. Experimental data were analyzed using the NNLS algorithm provided by the manufacturer.

CD Spectroscopy. The peptide secondary structure was monitored by CD spectroscopic measurement using a Jasco J-720 instrument (Tokyo, Japan). An optical cell with a 1 mm path length was used. Far-UV spectra at 25 °C were measured at a scan speed of 20 nm/min.

Fluorescence Assays for Amyloid Fibril Formation. Amyloid fibril formations of Aβ(1−40) (100 μg/mL) at 25 °C and tau 3RMBD (300 μg/mL) at 37 °C were assayed using fluorescence intensity of 20 μM thioflavin T (ThT). These assays were conducted in 50 mM sodium phosphate buffer (pH 7.5) containing 100 mM NaCl. The fluorescence assay of amyloid fibril formation was carried out using a Genios plate reader (TECAN). Fluorescence intensity measurements were performed with an excitation at 450 nm and emission at 485 nm in a 96-microwell plate as described previously.[12] Fluorescence intensity of 20 μM ThT was used to monitor

dx.doi.org/10.1021/bi3004236 | Biochemistry 2012, 51, 5394−5401

fibril formation of Aβ(1−40) (100 μg/mL) with 200 rpm shaking at 25 °C. Similarly, the fluorescence of ThT was used to assess fibril formation of tau 3RMBD (300 μg/mL) at 37 °C. Thioflavin S is commonly used as a fluorescence probe for fibril formation of tau 3RMBD. However, the αAC(71−88) amyloid induces coagulation, and so we did not use this assay.

RESULTS

Chaperone-like Activity of the αAC(71−88) Amyloid. Alcohol dehydrogenase (ADH), which has a pI of 5.4, has been used as a model chaperone substrate of crystallin and its peptide fragments in previous investigations.[9,27] The effect of fibril formation of αAC(71−88) on its chaperone-like activity was therefore studied by analyzing the thermal aggregation of ADH. In previous studies, the thermal aggregation of ADH was conducted at 48 °C. However, we found that at this temperature αAC(71−88) exhibited a conformational change from random coil to a β-strand (Figure S1) followed by the formation of amyloid fibrils. Thus, in order to assay the chaperone-like activity of the nonfibril αAC(71−88), the thermal aggregation of ADH was conducted at 44 °C, where the conformational change of αAC(71−88) is not induced for several hours. The turbidity change of a solution of ADH (150 μg/mL) at 44 °C (Figure 2, ○ plot) indicated a gradual buildup of ADH aggregates. TEM measurements showed that ADH formed amorphous aggregates in the size range 0.2−2 μm (Figure 1b). Moreover, these findings agree with the results of DLS analysis (Figure S2). A previous study showed that the aggregation of ADH at 50 °C was accompanied by enzymatic inactivation.[27] We found that the enzymatic activity of ADH after heat treatment at 44 °C was the same as that of native ADH. This finding indicates that heat treatment under these conditions does not induce irreversible inactivation of the enzyme. Hence, ADH aggregates formed at 44 °C were generated by reversible self-association of ADH. These aggregates subsequently dissociated into the native conformation when the ADH solution was diluted in buffer used for the enzymatic assay.

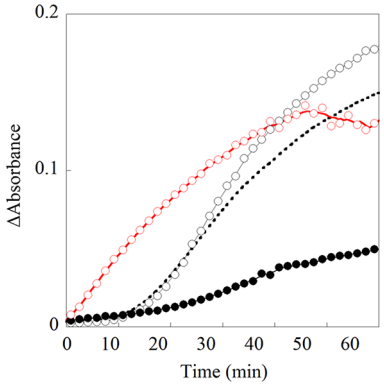

Figure 2. Effect of amyloid fibril on the aggregation of ADH. Kinetic changes in the turbidity of ADH (150 μg/mL) in 10 mM sodium phosphate (pH 7.5) with 100 mM NaCl at 44 °C. ○, no additives; ●, +10 μg/mL αAC(71−88) amyloid; dotted line, +10 μg/mL nonfibril αAC(71−88); red ○, +10 μg/mL Aβ(25−35) amyloid.

The nonfibril αAC(71−88) decelerated the aggregation of ADH (Figure 2, dotted plot), but the αAC(71−88) amyloid, which was prepared by thermal treatment of αAC(71−88) at 60 °C, had a much greater effect on the aggregation process at 44 °C (Figure 2, ● plot). This result indicates that the chaperone-like activity of αAC(71−88) using the aggregation of ADH as a model system is enhanced when the peptide forms amyloid fibrils. The chaperone-like activities of the nonfibril αAC(71−88) and the αAC(71−88) amyloid against 150 μg/mL ADH was increased with the increase of the peptide concentrations in the range of 10−100 μg/mL. In this concentration range, the activity of the αAC(71−88) amyloid was always higher than that of the same concentration of the nonfibril αAC(71−88). The change in the turbidity of the solution of ADH in the presence of αAC(72−88) was almost the same as that in the presence of nonfibril αAC(71−88), indicating that the removal of F71 from αAC(71−88) does not significantly affect the chaperone-like activity of the peptide. Therefore, F71 of αAC(71−88) is crucial for the chaperone-like activity of αAC(71−88) because of its contribution in promoting amyloid fibril formation.

The effect of the αAC(71−88) amyloid on the thermal aggregation of ADH was investigated by monitoring the concentration change of soluble ADH in solution. A mixture of ADH (150 μg/mL) and the αAC(71−88) amyloid (10 μg/mL) was incubated at 44 °C, and the concentration of soluble ADH was determined from the A_{280} absorbance after removal of aggregates by centrifugation. The observed rate of decrease in the concentration of soluble ADH in the presence and absence of the αAC(71−88) amyloid was the same (Figure S3), indicating that the interaction between native ADH and the αAC(71−88) amyloid is negligible. By contrast, TEM images of a mixed solution of ADH and the αAC(71−88) amyloid showed that small amorphous aggregates of ADH (size range of ca. 50−100 nm) were attached to the surface of the fibrils (Figure 1c). The larger aggregates of ADH in the range of ca. 1−2 μm were not detected.

We studied the effect of the αAC(71−88) amyloid on the aggregation of firefly luciferase (pI = 6.8), a model substrate for studying chaperone-assisted protein folding, by turbidity measurement. The turbidity change of a solution of luciferase (50 μg/mL) at 37 °C (Figure 3a, ○ plot) indicated a gradual buildup of luciferase aggregates. The nonfibril αAC(71−88) was found to decelerate the aggregation of luciferase (Figure 3a, dotted plot), although the αAC(71−88) amyloid decelerated the aggregation even more effectively (Figure 3a, ● plot). The chaperone-like activities of the nonfibril αAC(71−88) and the αAC(71−88) amyloid against 50 μg/mL luciferase were enhanced by increased concentrations of peptide in the range 2−6 μg/mL. Within this concentration range, the activity of the αAC(71−88) amyloid was always higher than that of the same concentration of the nonfibril αAC(71−88).

The aggregation of luciferase is irreversible,[13] and the chaperone-like activity of the αAC(71−88) amyloid was monitored through the effect on the inactivation of luciferase. As shown in Figure 3b, the inactivation of luciferase was decelerated in the presence of the αAC(71−88) amyloid fibrils. TEM images of a mixed solution of the luciferase and the αAC(71−88) amyloid shows that the small amorphous aggregates of luciferase were clustered to the surface of the αAC(71−88) amyloid (Figure 1d). These results suggest that the αAC(71−88) amyloid binds the small aggregates of substrate proteins on the surface to exhibit the chaperone-like activity.

Zeta Potential of the Amyloid Fibrils. The electrophoretic mobility of the amyloid fibril[28] was measured by using a laser microscope to study the role of the surface charge on the

dx.doi.org/10.1021/bi3004236 | Biochemistry 2012, 51, 5394−5401

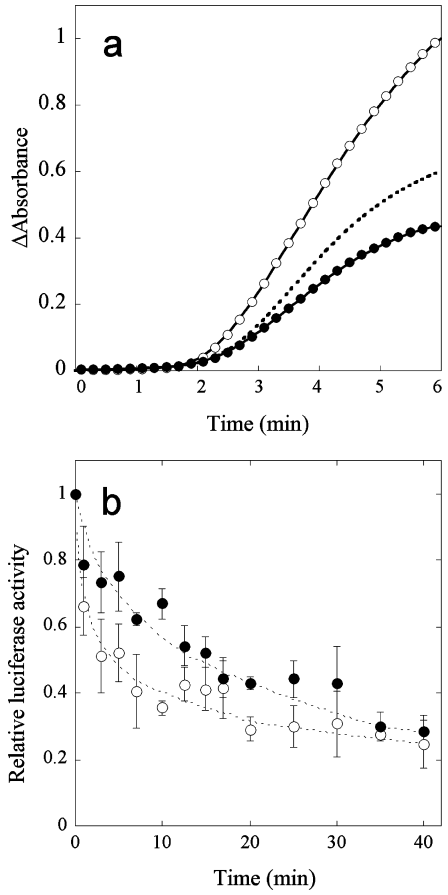

Figure 3. Effect of αAC(71−88) amyloid on the aggregation of firefly luciferase. (a) Kinetic changes in turbidity of luciferase (50 μg/mL) at 37 °C: ○, no additives; ●, +6 μg/mL αAC(71−88) amyloid; dotted line, +6 μg/mL nonfibril αAC(71−88). (b) Kinetics of the inactivation of the luciferase activity during the incubation at 37 °C: ○, no additives; ●, +6 μg/mL αAC(71−88) amyloid.

chaperone-like activity. The zeta potential value of the αAC(71−88) amyloid calculated from electrophoretic mobility was ca. −39 mV, indicating that the αAC(71−88) amyloid possesses an anionic surface. Because ADH and luciferase are both negatively charged at neutral pH, there is an electrostatic repulsion exerted between the αAC(71−88) amyloid and the protein aggregates.

The electrophoretic mobility of the amyloid fibrils preincubated with ADH at 44 °C was measured to study the effect of substrate binding on the surface charge of the amyloid. As shown in Figure 4 (○ plot), addition of up to 1 mg/mL ADH did not result in a significant change in the zeta potential value of αAC(71−88) amyloid. The magnitude of the zeta potential gives an indication of the stability of the colloidal system. A common dividing line between stable and unstable suspensions is generally taken at either +30 or −30 mV.[29] Therefore, the αAC(71−88) amyloid is stable as a colloidal dispersion and is unaffected by the binding of ADH.

To study the mechanism of the antichaperone activity of the amyloid fibrils, we measured electrophoretic mobility of the Aβ(25−35) amyloid, which exhibits antichaperone activity against acidic proteins via electrostatic attractions.[13] As shown by the red plot in Figure 2, the thermal aggregation of ADH was accelerated in the presence of the Aβ(25−35) amyloid, indicating an antichaperone activity. Electrophoretic mobility of

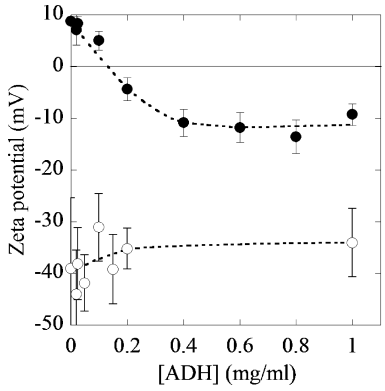

Figure 4. Zeta potential of the amyloid-substrate complex calculated from of the electrophoretic mobility. A mixture of amyloid (10 μg/mL) and various concentrations of ADH were incubated for 1 h at 44 °C. The solution was then diluted 25-fold before measuring the electrophoretic mobility. ○, αAC(71−88) amyloid; ●, Aβ(25−35) amyloid.

the Aβ(25−35) amyloid represented by a zeta potential value was ca. +9 mV, indicating an electrostatic attraction between Aβ(25−35) amyloid and ADH. The zeta potential of the Aβ(25−35) amyloid changed from ca. +9 mV to a negative value as the concentration of ADH increased from 0 to 1 mg/mL (Figure 4, ● plot). This result indicates that the positive charge on the surface of the Aβ(25−35) amyloid is canceled upon binding to anionic ADH, thereby reducing its colloidal stability. Thus, the mechanism by which amyloid fibrils modulate protein aggregation may be related to the colloidal stability.

Chaperone-like and Antichaperone Activity of the αAC(71−88) Amyloid. Given that there is an electrostatic repulsion exerted between the αAC(71−88) amyloid and its anionic substrate, the αAC(71−88) amyloid may bind the aggregates of ADH and luciferase via hydrophobic interactions. The amyloid surface was therefore analyzed using the fluorescence probe 1-anilino-8-naphthalenesulfonate (ANS). ANS is only slightly fluorescent in water (Figure 5, dotted line), but its spectrum is blue-shifted and its intensity significantly increased when it binds to nonpolar sites of polypeptides. The fluorescence emission of ANS increased in the presence of the αAC(71−88) amyloid with a concomitant blue-shift of its

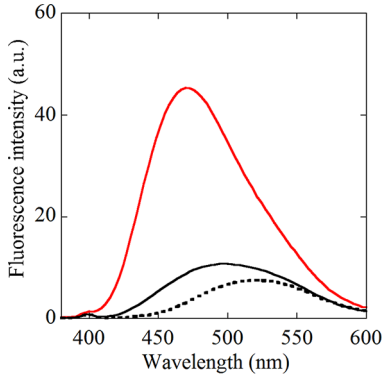

Figure 5. Fluorescence intensity of ANS in the presence of the amyloid fibril. Fluorescence spectra of 90 μM ANS was measured in 10 mM sodium phosphate (pH 7.5) with 100 mM NaCl at 37 °C. Dotted line, no additives; red line, +30 μg/mL αAC(71−88) amyloid; black solid line, +30 μg/mL Aβ(25−35) amyloid.

dx.doi.org/10.1021/bi3004236 | Biochemistry 2012, 51, 5394−5401

maximum fluorescence emission (Figure 5, red line). This result indicates that the surface of the αAC(71−88) amyloid comprises a hydrophobic environment.

Next, we examined the role of the electrostatic attraction between αAC(71−88) amyloid and a cationic substrate in terms of its antichaperone activity. This was done by analyzing the effect of αAC(71−88) amyloid on the heat-induced aggregation of hen egg white lysozyme (pI = 11.0). The amount of the heat-induced aggregates of lysozyme (230 μg/mL) produced at 98 °C in the presence and absence of the amyloid fibril was measured as described previously.[26] In the absence of amyloid fibril, there was a gradual increase in the fraction of aggregated lysozyme with incubation time (Figure 6,

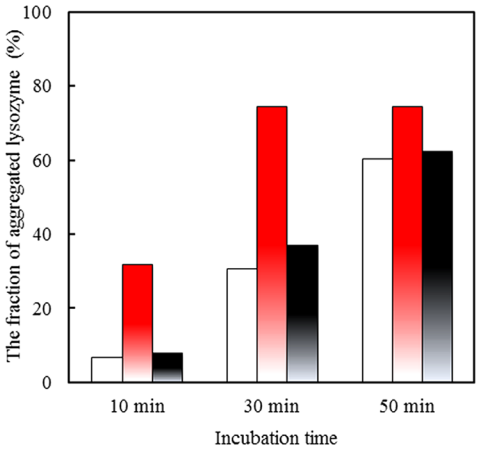

Figure 6. Amount of heat-induced aggregate of lysozyme produced at 98 °C. Solutions of lysozyme (230 μg/mL) in the presence or absence of amyloid fibril in pH 6.5 buffer were heated at 98 °C for 10, 30, or 50 min. After heat treatment, the concentration of soluble lysozyme was determined from the A_{280} of the solution after centrifugation. This value was used to calculate the amount of aggregation. White bar, no additives; red bar, +40 μg/mL αAC(71−88) amyloid; black bar, +40 μg/mL Aβ(25−35) amyloid.

white bar). The presence of αAC(71−88) amyloid (40 μg/mL) significantly increased the aggregation of lysozyme (Figure 6, red bar), which contrasts with the results for ADH and luciferase. This finding suggests that the antichaperone activity of αAC(71−88) amyloid is triggered by the canceling of the surface charge upon binding to its substrate.

The effect of the Aβ(25−35) amyloid on the heat-induced aggregation of lysozyme was also studied. As shown by the black bar in Figure 6, the Aβ(25−35) amyloid did not facilitate the aggregation of lysozyme, which supports our hypothesis that electrostatic attraction between amyloid and protein induces antichaperone activity. The amount of heat-induced aggregate of lysozyme was unaffected by the presence of the Aβ(25−35) amyloid, indicating the peptide does not exhibit chaperone-like or antichaperone activity. The absence of chaperone-like activity of the Aβ(25−35) amyloid can be explained by its low surface hydrophobicity. Indeed, this can be seen from the fluorescence emission of ANS in the presence of the Aβ(25−35) amyloid, which does not show a significant blue-shift or increase of intensity (Figure 5, black solid line).

Design of an Amyloid Fibril To Prevent the Fibril Formation in Pathological Proteins. Next, we examined the potential application of the αAC(71−88) amyloid in preventing the onset of neurodegenerative disorders. Specifically, we analyzed the effect of the αAC(71−88) amyloid on fibril formation of two pathological proteins of Alzheimer's disease, amyloid β protein,[30] and tau protein.[31] Alzheimer's disease is thought to initially develop from extracellular deposits of amyloid β that trigger a cascade leading to the intracellular accumulation of phosphorylated tau and a subsequent loss of neuronal cells.[32] Previous studies have shown that amyloid fibril formation of a fragment of amyloid β Aβ(1−40), which has a pI of 5.5, is suppressed by αAC(71−88) and its derivatives.[12,33] We confirmed that the αAC(71−88) amyloid also exhibits the chaperone-like activity against the fibril formation of Aβ(1−40) using a ThT fluorescence assay (Figure S4).

The chaperone-like activity of the αAC(71−88) amyloid against fibril formation of tau was examined by using a model protein comprising three-repeats of a microtubule-binding domain (3RMBD; pI = 9.6).[24,34] Incubation of tau 3RMBD (300 μg/mL) at 25 °C resulted in a gradual increase in the intensity of ThT fluorescence (Figure 7a, ○ plot), indicating a

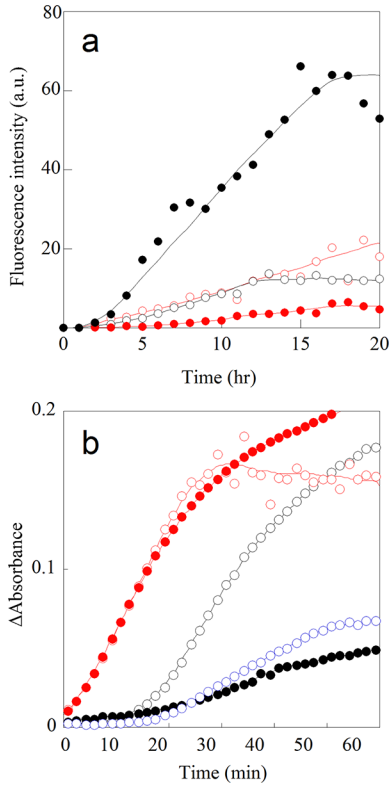

Figure 7. Effect of the amyloid fibril of the αAC(71−88) variants on the protein aggregation. (a) Time course of ThT fluorescence intensity of solutions of tau 3MBD (300 μg/mL) incubated at 25 °C: ○, no additives; ●, +60 μg/mL αAC(71−88) amyloid; red ○, +60 μg/mL αAC(71−88)2K amyloid; red ●, +60 μg/mL the αAC(71−88)3K amyloid. (b) Kinetic changes in the turbidity of ADH (150 μg/mL) at 44 °C: ○, no additives; ●, +αAC(71−88) amyloid; blue ○, +10 μg/mL αAC(71−88)1K; red ○, +10 μg/mL αAC(71−88)2K amyloid; red ●, +10 μg/mL the αAC(71−88)3K amyloid.

slow growth of fibrils. However, there was a marked acceleration in the increase of ThT fluorescence in the presence of the αAC(71−88) amyloid (Figure 7a, ● plot). These results suggest that the αAC(71−88) amyloid facilitates fibril formation of tau 3RMBD. 3RMBD is a cationic protein and is readily polymerized into amyloid fibrils in the presence of polyanions.[35] Hence, our results can be explained by the antichaperone activity of the αAC(71−88) amyloid, which

dx.doi.org/10.1021/bi3004236 | Biochemistry 2012, 51, 5394−5401

compensates for the positive charges of 3RMBD to induce aggregation.

Variants of αAC(71−88) were designed in order to obtain amyloid fibrils with chaperone activity against the fibril formation of tau. Ser81, Glu83, and Leu86, the nonconserved amino acids in the crystallin family[36] of αAC(71−88), were substituted to Lys to obtain αAC(71−88)1K, -2K, and -3K (Table 1). TEM analysis showed that all of these αAC(71−88) peptides form regular fibrils. Electrophoretic mobility measurements indicated that amyloid fibrils formed from the 2K and 3K mutants possess a positively charged surface, while the αAC(71−88) 1K amyloid is negatively charged as shown by the zeta potential values given in Table 1. Figure 7b shows the turbidity change of ADH aggregation in the presence of amyloid fibrils of the αAC(71−88) variants. Although the negatively charged amyloid fibril of 1K mutant showed chaperone-like activity (Figure 7b, blue plot), the amyloid fibrils of 2K and 3K mutants accelerated the rate of aggregation of ADH (Figure 7b, red plot).

Table 1. Sequence of αAC(71-88), Variants, and Aβ(25-35) and Their Zeta Potential Value at Neutral pH

	sequence	zeta potential of amyloid fibril (mV)
αAC(71−88)	FVIFLDVKHFSPEDLTVK	−39.1 ± 8.0
αAC(71−88)1K	FVIFLDVKHFSPEDL*K*VK	−22.5 ± 3.2
αAC(71−88)2K	FVIFLDVKHFSP*K*DL*K*VK	+19.4 ± 2.0
αAC(71−88)3K	FVIFLDVKHF*K*P*K*DL*K*VK	+20.0 ± 2.8
Aβ(25−35)	GSNKGAIIGLM	+8.8 ± 1.6

These results indicate that electrostatic attraction between the cationic amyloid fibrils of αAC(71−88) variants and the anionic ADH promotes aggregation, which is consistent with our mechanism for antichaperone activity. We also examined the effect of amyloid fibrils of 2K and 3K mutants on fibril formation. Our results show that these cationic αAC(71−88) amyloids did not facilitate fibril formation (Figure 7a, red plots). The same plots demonstrate that the αAC(71−88)3K amyloid suppresses fibril formation of 3RMBD. TEM analysis of solutions of tau in the presence of αAC(71−88)3K amyloid show that the small amorphous aggregates of tau (ca. 50−100 nm) attach to the surface of the fibrils (Figure 8). Therefore, the αAC(71−88)3K amyloid exhibits chaperone-like activity against fibril formation of tau by trapping small aggregates of 3RMBD.

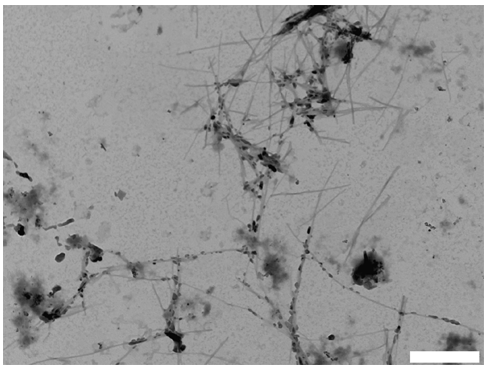

Figure 8. TEM images of aggregates obtained by the incubation of a mixture of tau 3MRD (29 μg/mL) and the αAC(71−88)3K amyloid (29 μg/mL) at 37 °C for 1 h.

DISCUSSION

The αAC(71−88) amyloid exhibited chaperone-like activity to impede the aggregation of anionic substrates. By contrast, aggregation of the same proteins was promoted by the Aβ(25−35) amyloid. Heat-induced aggregation of a cationic substrate was facilitated by the αAC(71−88) amyloid. Measurement of the zeta potential of the amyloid fibril revealed that its surface charge plays a significant role in terms of the modulation of the protein aggregation. The zeta potential value of the αAC(71−88) amyloid calculated from electrophoretic mobility was ca. −39 mV, and this large negative zeta potential value indicates that αAC(71−88) amyloid is stable as a colloidal dispersion. By contrast, the zeta potential of the Aβ(25−35) amyloid was ca. +9 mV, and binding to the negatively charged ADH changed this positive zeta potential to a negative value.

The binding between the protein aggregates and the amyloid fibrils via electrostatic attraction cancels the surface charge of the amyloid and therefore reduces colloidal stability, inducing the formation of large coagulates of amyloid (Figure 9). When the amyloid fibrils coagulate to form large aggregates, the small aggregates of substrate do not dissociate from the surface of the amyloid. The subsequent cascade in the growth of coagulation results in an increase in the amount of irreversible aggregation of substrate. These results indicate that one of the key factors determining whether amyloid fibrils display chaperone-like or antichaperone activity is their colloidal stability which is affected by the electrostatic interaction with the substrate.

α-Crystallin and the related peptide αAC(71−88) prevent protein aggregation by providing a suitable spatial arrangement of hydrophobic surfaces.[9] Similar results have been reported for the isolated substrate binding domain of *Escherichia coli* molecular chaperones,[18−23] which exhibit chaperone-like activity against various substrates. Although the chaperone-like activity of the substrate binding domain of GroEL was less than that of the intact protein, it was significantly improved when the binding domains were assembled on a heptameric ring.[21] Similarly, the chaperone-like activity of αAC(71−88), which is less than that of intact α-cystallin, was enhanced when it formed an amyloid fibril. The chaperone-like activity of the N-terminal substrate binding domain of ClpB is best explained in terms of weak binding to a reversible aggregate of substrate via hydrophobic interactions.[23] Likewise, we found that the αAC(71−88) amyloid may bind the aggregates of ADH and luciferase via hydrophobic interactions because the surface of the αAC(71−88) amyloid comprises a hydrophobic environment. This result indicates that we can interpret the chaperone-like activity of the αAC(71−88) amyloid by an analogous mechanism to that of the substrate binding domain of molecular chaperones. Thus, a large continuous surface of amyloid fibril facilitates a series of weak hydrophobic interactions with the substrate, thereby increasing the affinity of binding. The chaperone-like activity of the αAC(71−88) amyloid against the inactivation of luciferase may be explained by Scheme 1.

Peptides that display chaperone-like activity have potential clinical applications in preventing the onset of diseases related to protein misfolding.[37−39] Here, we designed amyloid fibrils of αAC(71−88) and its derivatives that prevent amyloid fibril formation of two pathological proteins associated with Alzheimer's disease. The fibril formation of the negatively charged Aβ(1−40) was inhibited by the αAC(71−88) amyloid,

dx.doi.org/10.1021/bi3004236 | *Biochemistry* 2012, 51, 5394−5401

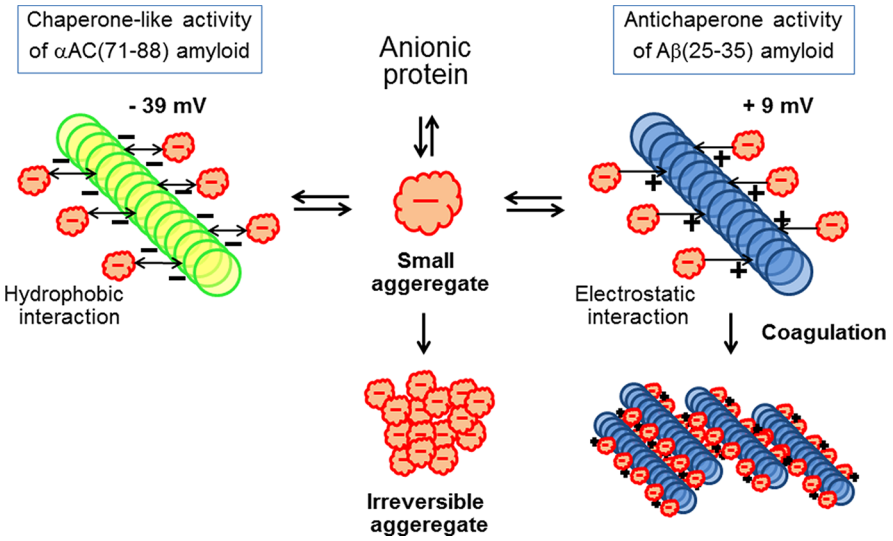

Figure 9. Hypothetical scheme of events following the interaction between the amyloid fibrils and protein aggregates.

Scheme 1

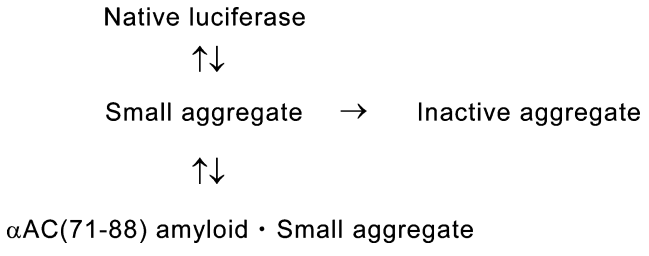

and that of the positively charged tau was suppressed by the cationic amyloid of αAC(71−88) variants. Thus, αAC(71−88) and its derivatives represent promising novel peptide drug candidates with a self-assembly function for preventing neurodegenerative disorders. Moreover, recent developments that allow peptide drug delivery across the blood−brain barrier could be exploited to facilitate appropriate targeting of αAC(71−88) and its derivatives.[40]

Previous studies suggest that protein aggregation induced by the Aβ(25−35) amyloid may damage a wide range of biological systems by inactivating numerous enzymes in the cell as well as in the extracellular matrix.[13] Similarly, αAC(66−80) (SDRDKFVIFLDVKHF), a fragment of αA-crystallin that accumulates in the aging lens, can cause cataracts by possibly disrupting the structure and organization of crystallins via its antichaperone activity.[15] αAC(66−80) forms amyloid fibrils under physiological conditions. We found that αAC(66−80) amyloid is prone to coagulate because of its low surface charge (pI = 7.36). These results suggest that a modulation in the colloidal stability may play a significant role in the mechanism of the antichaperone activity of these amyloid fibrils. This novel mechanism could explain the development of various diseases caused by protein aggregation.

■ ASSOCIATED CONTENT

Supporting Information

Experimental results of the effect the secondary structure of αAC(71−88) at 44 °C, the size of the heat-induced aggregate of ADH, the effect of the αAC(71−88) amyloid on the concentration of nonaggregated ADH, and the effect of the αAC(71−88) amyloid on the fibril formation of Aβ(1−40). This material is available free of charge via the Internet at http://pubs.acs.org.

■ AUTHOR INFORMATION

Corresponding Author

*Fax +81-75-724-7861; e-mail tanaka@kit.ac.jp.

Funding

This work was supported by Grant-in-Aid for Scientific Research (No. 20550111) from the Japanese Ministry of Education, Culture, Sports, Science and Technology, and Adaptable and Seamless Technology Transfer Program through Target-driven R&D (No. AS231Z00074G) from Japan Science and Technology Agency.

Notes

The authors declare no competing financial interest.

■ ABBREVIATIONS

αAC, αA-crystallin; ADH, alcohol dehydrogenase; ANS, 1-anilino-8-naphthalenesulfonate; Aβ, amyloid β; 3RMBD, three-repeat microtubule-binding domain; ThT, thioflavin T.

■ REFERENCES

(1) Dobson, C. M. (2003) Protein folding and misfolding. *Nature 426*, 884−890.

(2) Broersen, K., Rousseau, F., and Schymkowitz, J. (2010) The culprit behind amyloid beta peptide related neurotoxicity in Alzheimer's disease: oligomer size or conformation? *Alzheimer's Res. Ther. 2*, 12.

(3) Clark, J. I., and Muchowski, P. J. (2000) Small heat-shock proteins and their potential role in human disease. *Curr. Opin. Struct. Biol. 10*, 52−59.

(4) Horwitz, J. (2003) Alpha-Crystallin. *Exp. Eye Res. 76*, 145−153.

(5) Laganowsky, A., Benesch, J. L., Landau, M., Ding, L., Sawaya, M. R., Cascio, D., Huang, Q., Robinson, C. V., Horwitz, J., and Eisenberg, D. (2010) Crystal structures of truncated alphaA and alphaB crystallins reveal structural mechanisms of polydispersity important for eye lens function. *Protein Sci. 19*, 1031−1043.

(6) Raman, B., and Rao, C. M. (1997) Chaperone-like activity and temperature-induced structural changes of alpha-Crystallin. *J. Biol. Chem. 272*, 23559−23564.

(7) Sharma, K. K., Kumar, G. S., Murphy, A. S., and Kester, K. (1998) Identification of 1,1′-bi(4-anilino)naphthalene-5,5′-disulfonic acid

binding sequences in alpha-Crystallin. *J. Biol. Chem. 273*, 15474–15478.
(8) Santhoshkumar, P., and Sharma, K. K. (2001) Phe71 is essential for chaperone-like function in alpha A-Crystallin. *J. Biol. Chem. 276*, 47094–47099.
(9) Sharma, K. K., Kumar, R. S., Kumar, G. S., and Quinn, P. T. (2000) Synthesis and characterization of a peptide identified as a functional element in alphaA-Crystallin. *J. Biol. Chem. 275*, 3767–3771.
(10) Bhattacharyya, J., Padmanabha Udupa, E. G., Wang, J., and Sharma, K. K. (2006) Mini-alphaB-Crystallin: a functional element of alphaB-Crystallin with chaperone-like activity. *Biochemistry 45*, 3069–3076.
(11) Ghosh, J. G., Estrada, M. R., and Clark, J. I. (2005) Interactive domains for chaperone activity in the small heat shock protein, human alphaB Crystallin. *Biochemistry 44*, 14854–14869.
(12) Tanaka, N., Tanaka, R., Tokuhara, M., Kunugi, S., Lee, Y. F., and Hamada, D. (2008) Amyloid fibril formation and chaperone-like activity of peptides from alphaA-Crystallin. *Biochemistry 47*, 2961–2967.
(13) Konno, T. (2001) Amyloid-induced aggregation and precipitation of soluble proteins: an electrostatic contribution of the Alzheimer's beta(25–35) amyloid fibril. *Biochemistry 40*, 2148–2154.
(14) Olzscha, H., Schermann, S. M., Woerner, A. C., Pinkert, S., Hecht, M. H., Tartaglia, G. G., Vendruscolo, M., Hayer-Hartl, M., Hartl, F. U., and Vabulas, R. M. (2011) Amyloid-like aggregates sequester numerous metastable proteins with essential cellular functions. *Cell 144*, 67–78.
(15) Santhoshkumar, P., Raju, M., and Sharma, K. K. (2011) alphaA-Crystallin peptide SDRDKFVIFLDVKHF accumulating in aging lens impairs the function of alpha-Crystallin and induces lens protein aggregation. *PLoS One 6*, e19291.
(16) Derjaguin, B., and Landa, L. (1941) Theory of the stability of strongly charged lyophobic sols and of the adhesion of strongly charged particles in solution of electrolytes. *Acta Physicochim. URSS 14*, 633–662.
(17) Verwey, E. J., and Overbeek, J. T. G. (1948) *Theory of the Stability of Lyophobic Colloids*, Elsevier, New York.
(18) Zahn, R., Buckle, A. M., Perrett, S., Johnson, C. M., Corrales, F. J., Golbik, R., and Fersht, A. R. (1996) Chaperone activity and structure of monomeric polypeptide binding domains of GroEL. *Proc. Natl. Acad. Sci. U.S.A. 93*, 15024–15029.
(19) Chatellier, J., Buckle, A. M., and Fersht, A. R. (1999) GroEL recognises sequential and non-sequential linear structural motifs compatible with extended beta-strands and alpha-helices. *J. Mol. Biol. 292*, 163–172.
(20) Tanaka, N., and Fersht, A. R. (1999) Identification of substrate binding site of GroEL minichaperone in solution. *J. Mol. Biol. 292*, 173–180.
(21) Chatellier, J., Hill, F., and Fersht, A. R. (2000) From Minichaperone to GroEL 2: Importance of Avidity of the Multisite Ring Structure. *J. Mol. Biol. 304*, 883–896.
(22) Tanaka, N., Nakao, S., Wadai, H., Ikeda, S., Chatellier, J., and Kunugi, S. (2002) The substrate binding domain of DnaK facilitates slow protein refolding. *Proc. Natl. Acad. Sci. U.S.A. 99*, 15398–15403.
(23) Tanaka, N., Tani, Y., Hattori, H., Tada, T., and Kunugi, S. (2004) Interaction of the N-terminal domain of Escherichia coli heat-shock protein ClpB and protein aggregates during chaperone activity. *Protein Sci. 13*, 3214–3221.
(24) Okuyama, K., Nishiura, C., Mizushima, F., Minoura, K., Sumida, M., Taniguchi, T., Tomoo, K., and Ishida, T. (2008) Linkage-dependent contribution of repeat peptides to self-aggregation of three- or four-repeat microtubule-binding domains in tau protein. *FEBS J. 275*, 1529–1539.
(25) Yao, T. M., Tomoo, K., Ishida, T., Hasegawa, H., Sasaki, M., and Taniguchi, T. (2003) Aggregation analysis of the microtubule binding domain in tau protein by spectroscopic methods. *J. Biochem. 134*, 91–99.
(26) Kudou, M., Shiraki, K., Fujiwara, S., Imanaka, T., and Takagi, M. (2003) Prevention of thermal inactivation and aggregation of lysozyme by polyamines. *Eur. J. Biochem. 270*, 4547–4554.
(27) Guagliardi, A., Cerchia, L., and Rossi, M. (1995) Prevention of in vitro protein thermal aggregation by the Sulfolobus solfataricus chaperonin. Evidence for nonequivalent binding surfaces on the chaperonin molecule. *J. Biol. Chem. 270*, 28126–28132.
(28) Jones, O. G., Adamcik, J., Handschin, S., Bolisetty, S., and Mezzenga, R. (2010) Fibrillation of beta-lactoglobulin at low pH in the presence of a complexing anionic polysaccharide. *Langmuir 26*, 17449–17458.
(29) Fast, J. L., Cordes, A. A., Carpenter, J. F., and Randolph, T. W. (2009) Physical instability of a therapeutic Fc fusion protein: domain contributions to conformational and colloidal stability. *Biochemistry 48*, 11724–11736.
(30) Selkoe, D. J. (1996) Amyloid beta-protein and the genetics of Alzheimer's disease. *J. Biol. Chem. 271*, 18295–18298.
(31) Goedert, M., Klug, A., and Crowther, R. A. (2006) Tau protein, the paired helical filament and Alzheimer's disease. *J. Alzheimer's Dis. 9*, 195–207.
(32) Tanzi, R. E., and Bertram, L. (2005) Twenty years of the Alzheimer's disease amyloid hypothesis: a genetic perspective. *Cell 120*, 545–555.
(33) Santhoshkumar, P., and Sharma, K. K. (2004) Inhibition of amyloid fibrillogenesis and toxicity by a peptide chaperone. *Mol. Cell. Biochem. 267*, 147–155.
(34) Wille, H., Drewes, G., Biernat, J., Mandelkow, E. M., and Mandelkow, E. (1992) Alzheimer-like paired helical filaments and antiparallel dimers formed from microtubule-associated protein tau in vitro. *J. Cell Biol. 118*, 573–584.
(35) Friedhoff, P., von Bergen, M., Mandelkow, E. M., Davies, P., and Mandelkow, E. (1998) A nucleated assembly mechanism of Alzheimer paired helical filaments. *Proc. Natl. Acad. Sci. U.S.A. 95*, 15712–15717.
(36) de Jong, W. W., Caspers, G. J., and Leunissen, J. A. (1998) Genealogy of the alpha-Crystallin small heat-shock protein superfamily. *Int. J. Biol. Macromol. 22*, 151–162.
(37) Friedler, A., Hansson, L. O., Veprintsev, D. B., Freund, S. M. V., Rippin, T. M., Nikolova, P. V., Proctor, M. R., Rüdiger, S., and Fersht, A. R. (2002) A peptide that binds and stabilizes p53 core domain: Chaperone strategy for rescue of oncogenic mutants. *Proc. Natl. Acad. Sci. U.S.A. 99*, 937–942.
(38) Reches, M., Porat, Y., and Gazit, E. (2002) Amyloid Fibril Formation by Pentapeptide and Tetrapeptide Fragments of Human Calcitonin. *J. Biol. Chem. 277*, 35475–35480.
(39) Zhou, A., Stein, P. E., Huntington, J. A., Sivasothy, P., Lomas, D. A., and Carrell, R. W. (2004) How small peptides block and reverse serpin polymerisation. *J. Mol. Biol. 342*, 931–941.
(40) Brasnjevic, I., Steinbusch, H. W., Schmitz, C., and Martinez-Martinez, P. (2009) Delivery of peptide and protein drugs over the blood-brain barrier. *Prog. Neurobiol. 87*, 212–251.